Metal Vapors in Gas Tungsten Arcs: Part I. Spectroscopy and Monochromatic Photography

G. J. DUNN, C. D. ALLEMAND, and T. W. EAGAR

Metal vapors in gas tungsten welding arcs were studied in order to determine the effects of these vapors on arc properties and subsequently on weld bead configuration. Emission spectroscopy and monochromatic photography were used to determine the prominent metal species present and their distribution in arcs on stainless steel. It was found that, in addition to the expected species (Fe, Mn, Cr), calcium and aluminum vapors were also detectable, although these elements were present in the base plate only at very low concentrations. All metal vapors were determined to be concentrated just above the weld pool in high current arcs, but were also detected in the upper regions of low current arcs. Aluminum, calcium, and sometimes thorium were found to vaporize from the tungsten electrode.

I. INTRODUCTION

A longstanding problem in GTA welding is the variation in weldability between different heats of the same metal. With increasing automation, it is desirable to obtain consistent weld quality with a single set of weld parameters.

It is believed by many investigators[1-11] that these variations in weldability are a result of varying concentrations of minor elements in the material. These elements may vaporize and enter the arc, thus affecting its characteristics. To develop an understanding of such phenomena, it is first necessary to experimentally measure vapor concentrations in welding arcs, and to correlate these concentrations with observed weld behavior.

In this study, emission spectroscopy was used to determine which metallic vapor spectra are dominant in the welding arc. Monochromatic photography was used to determine the distribution of these vapors in the arc. In Part II of this report, theoretical calculations of the effects of these elements on arc transport properties will be discussed.

II. PREVIOUS WORK

The effects of minor elements on the weldability of various basemetals have been reviewed up to 1976 by Glickstein and Yeniscavich.[1]

In 1968 Ludwig[2] reported finding variable penetration and skewed welds between two different heats of 304 stainless steel. He attributed this to the concentration of easily ionized impurities in the basemetal, in particular the alkali and alkaline-earth elements "of which calcium is strongly suspected." Moisio and Leinonen[3] reported similar results with heats of 304 and 316 stainless steels, and noted that, in a butt weld between two steels of different weldability, the arc was strongly attracted to the side of the steel which exhibited a lower depth-to-width ratio. Metcalfe and Quigley[4] explained this type of phenomenon in their studies on stainless steel as a propensity of the arc to move toward the material with a higher concentration of Al and Mn.

Oyler, *et al.*[5] cited a preferred composition of Si and Mn in 304L stainless steel for increased penetration. Savitskii and Leskov[6] found that "smaller depths of penetration and greater weld widths always corresponded to reduced amounts of sulfur and oxygen in the steel, and increased amounts of calcium." Bennett and Mills[7] argue that an increased amount of aluminum in the weld metal seems to "interact with manganese to produce increased Mn in the arc." This in turn was believed to be the cause of decreased penetration. Patterson[8] found that poor penetration in high Mn austenitic stainless steels blamed on aluminum content could be improved by titanium additions. Republic Steel[9] has correlated improved weld penetration in AOD refined stainless steels with increased carbon and sulfur content and decreased silicon content. Of these, sulfur had by far the greatest effect.

Savage, *et al.*[10,11] investigated the effects of 64 possible combinations of sulfur, phosphorus, silicon, manganese, titanium, and aluminum powder inserts in INCONEL 600.*

*INCONEL is a trademark of the INCO family of companies.

Increased penetration and weld cross-sectional areas were recorded for additions of Si, Ti, and P, and negative effects for Al. In another paper,[12] Savage reports that small increases in the amount of oxygen and nitrogen impurities in the argon shielding gas produced significantly decreased weld penetration.

Many researchers[1,2,4,6,13,14] believe that the significant property of basemetal impurities is the ionization potential. Most metallic elements have ionization potentials ½ to ⅓ that of argon (Table I);[15] thus, even small amounts of metal vapor in the arc can significantly affect the arc configuration and current density distribution and, consequently, the energy input to the workpiece.[13-14,16] Furthermore, it has been noted by Block-Bolten and Eagar[17] that "small changes in concentration of a minor element, A, in the melt may produce dramatic changes in the concentration of the element in the gas phase." This is due to the highly negative values of $\log a_A$ for log concentration of A, where a_A is the thermodynamic activity of species A, and is determined by the equation:

$$\ln \bar{p}_A = \ln p_A^\circ + \ln a_A$$

where p_A° = equilibrium vapor pressure of pure A
$\bar{p}_A$ = partial pressure of A above the alloy

G. J. DUNN is Materials Scientist, IBT, Beverly, MA. C. D. ALLEMAND, Consultant, and T. W. EAGAR, Associate Professor, are with Massachusetts Institute of Technology, Cambridge, MA 02139.

Manuscript submitted August 26, 1985.

Table I. First Ionization Potentials for Various Elements[15]

Element	V (eV)
He	24.581
Ar	15.755
W	7.98
Fe	7.87
Ni	7.633
Mn	7.432
Cr	6.764
Th	6.2
Ca	6.111
Al	5.984

Thus it can be seen that small variations in the concentration of trace elements in a metal can significantly affect the composition of metal vapor in the plasma.

Metcalfe and Quigley[4] calculated the contribution of metal vapors to the electron density, n_e, in the arc. However, it appears that the metal vapor density, n_a, was calculated from the vapor pressure of the pure element (p_A° above), not from the partial pressure $\overline{p}_A$ of the element in solution, which is a more correct measure of the concentration in the arc plasma.

Glickstein[13] has developed a one-dimensional model of the welding arc to study the effects of Al vapor on the radial temperature distribution (and consequently the current density distribution and energy input to the weldment). However, Block-Bolten and Eagar[17] have shown that Al will not be the dominant metal vapor species in the plasma, and they suggest that "the calculations performed by Glickstein would not produce such dramatic changes in plasma properties if a ternary addition, such as Mn, at 1000 times the Al concentration, were also added to the plasma gas." This point will be investigated in Part II of this paper.

A number of researchers have used emission spectroscopy to a limited extent in studying metal vapors in the arc. Savitskii and Leskov[6] studied the wavelength region between 240 and 250 nm, and identified Ca, Fe, Mn, Si, and C lines from arcs on high strength steels. They found that the introduction of an oxygen containing flux caused a decrease in the intensity of Ca, Fe, and Mn lines, and an increase in Si and C lines.

Glickstein[18] determined that Mn, Ni, and Cr vapors were present in arcs on Alloy 600. Shaw[19] was able to identify Ar, Fe, Cr, and possibly Mn lines in spectra taken from arcs on 304 stainless. Bennett and Mills[7] observed that, in arcs on high manganese stainless steels, Mn was the dominant vapor, followed by Cr, Fe, and Ni. Aluminum lines were also identified. Metcalfe and Quigley[4] noted that heats of steel which exhibited poor penetration produced spectra with more intense Mn ion lines. Key, *et al.*[20] observed that, in spectra of arcs on 304 stainless steel, manganese and chromium are the metal vapors which produce the most intense lines. They also noted that increasing the weld current or switching from argon to helium shielding gas increased the amount of metal vapor in the arc.

Spectra taken by Metcalfe and Quigley,[4] Glickstein,[18] and Quigley, *et al.*[21] indicate that the metal vapors are concentrated in a region very close to the anode, and that argon seems to dominate the upper region of the arc. Shaw[19] used monochromatic photography to determine the concentration of Cr vapor in the arc, and reported a bright patch of light just over the base plate. Mills,[22] using monochromatic video photography, noted that enhanced manganese vaporization was evident over weld pools on stainless steels which exhibited low depth-to-width ratios.

Ivanova[23] used spectroscopy to investigate the emission of vapors from thoriated, lanthanized, and yttriumized tungsten electrodes. He found substantial emissions of these elements during initial burning, decreasing to a background level after approximately twenty minutes.

Heiple and Roper[24–27] have investigated the effects of minor elements on weld pool motion. They have shown that surface-active elements such as sulfur and selenium, by producing a positive surface tension coefficient (increasing surface tension with increasing temperature), will cause the molten weld metal to flow from the pool's periphery to its center. This inward flow promotes efficient heat transfer to the weld root, thereby enhancing penetration. Similar findings have been reported by Makara, *et al.*[28] and a collaborative General Electric–Rensselaer Polytechnic Institute investigation.[29]

It can be seen that research devoted to studying minor element effects is extensive and has been a concern for some time. Nevertheless, it is also evident that a complete understanding of how minor element additions alter weld behavior has not yet been accomplished.

III. EXPERIMENTAL PROCEDURE

A. *Spectroscopy*

The spectroscopic measurements in this study were made with an apparatus constructed on rigid optical bars and carriages for maximum stability and versatility, and mounted on an optical bench. An automatically controlled moving weld table was employed so that the welding torch, and therefore the optical train, could remain stationary. This table was mounted on a sturdy optical jack for easy vertical adjustment. The torch was mounted on a two-dimensional translation stage with micrometer adjustments for precision positioning.

Light from the arc was focused by a lens onto the entrance slit (25 μm) of a Jarrell-Ash Mark X spectrograph. An iris diaphragm (3 mm diameter) and neutral density filter were used to reduce the amount of light which would ultimately strike the sensitive detector. Preliminary experiments indicated that metal vapor spectra were strongest in the light from the lower portion of the arc. Therefore, primarily a light from this area was analyzed. A Princeton Applied Research Corporation Model 1254 Silicon Intensified Target (SIT) vidicon detector was mounted at the exit port of the spectrograph. Only a 2.5 mm high band at the center of the 12.5 mm square SIT target was monitored in order to avoid peripheral effects due to aberrations inherent to the spectrograph and detector[30] which would result in increased linewidth and thus reduced resolution. The full width of the SIT target was monitored, however, allowing a 30 nm wavelength range of the spectrum to be viewed at one time. The image on this target could be viewed directly on an X-Y oscillographic monitor, allowing real-time observations of the weld spectrum.

Information from the detector is transferred to an Optical Multichannel Analyzer (OMA2). Spectra appear on a CRT

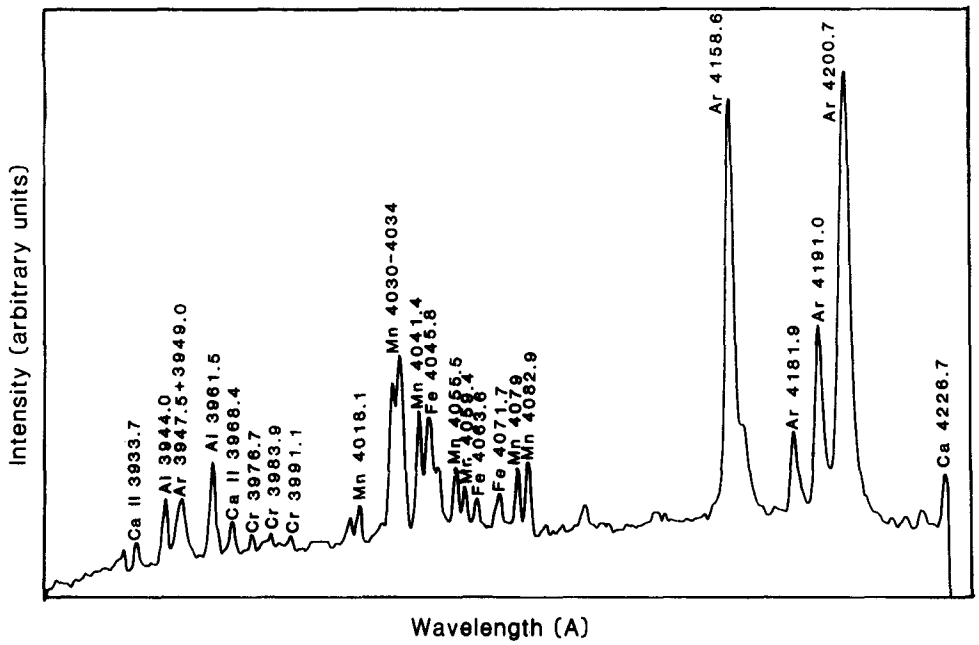

Fig. 1—Spectrum recorded from a 125 A arc on the standard 304 steel (W155).

as plots of intensity *vs* wavelength. The wavelength scale is a function of the spectrograph and grating used. It is therefore left to the investigator to calibrate this axis. In the present study, this was done with the use of atomic absorption hollow cathode tubes. Iron, manganese, chromium, calcium, aluminum, and argon spectra were recorded and identified.

B. *Monochromatic Photography*

Monochromatic photography was used in this study to determine the distribution of metal vapors in the welding arc. A reflective optics double monochromator[31] provided a monochromatic two-dimensional image of the arc; *i.e.*, only light of a very narrow wavelength range (~1.4 nm) is transmitted by the instrument. This range can be selected at characteristic wavelengths of the elements of interest, thereby producing a two-dimensional "mapping" of the distribution of any element in the welding arc.

Initial attempts to photograph the arc with multilayer thin film narrowband interference filters were unsuccessful due to the low light rejection ratios of these filters (on the order of 10^4). The total integrated intensity of the many strong argon and additional metal vapor lines can exceed the intensity of the spectral line of the element of interest by more than 10^4. The very high (approximately 10^8) light rejection of the double monochromator is required to eliminate the intense argon light and allow detection of the weaker metal vapor spectral lines.

C. *Welding Conditions*

In order to study the effects of different welding environments on vapor concentrations in the arc, various base plate compositions, shielding gases, and weld parameters were investigated. The weld metal primarily studied was stainless steel, which many researchers[2-5,7-9] have noted to exhibit heat-to-heat variations in weldability. Samples from three different heats of 304L were obtained from Republic Steel Corporation. The chemical compositions, as supplied by Republic, for these steels are given in Table II. Note that heat W155 is the base composition, heat W167A having a significantly greater calcium content, and heat W156 a greater sulfur content. Weld penetration studies were made on these steels by Republic,[9] and it was found that heat W156, high in sulfur, exhibited consistently improved penetration, whereas W167A, high in calcium, exhibited decreased penetration, although the results are somewhat less consistent. These findings are in agreement with those of previous studies.

Spectra were recorded from arcs on these steels over the full spectral range of the equipment (350 to 800 nm), and it was found that a single region between 380 and 426 nm contained the strongest lines of all of the elements of interest. Therefore, most studies were performed using this region of the spectrum. When greater resolution was desired, the second order of these lines was studied.

Tests were made on both traveling and stationary welds, with the bulk of the welds stationary. A 10 mm (±1 mm)

Table II. Compositions of the Republic Stainless Steel Heats

	Composition (Weight Percent)													
Heat	C	Mn	Si	P	S	Cr	Ni	Mo	V	Cu	Al	N	O	Ca
W155	0.020	1.7	0.48	0.027	0.005	18.20	9.5	0.37	<0.01	0.34	0.007	0.063	0.012	0.0004
W156	0.020	1.7	0.47	0.029	0.025	18.55	9.5	0.37	<0.01	0.34	0.007	0.070	0.011	0.0003
W167A	0.037	1.6	0.53	0.025	0.007	18.00	9.5	0.40	0.05	0.28	0.009	0.052	0.011	0.0080

arc length was used throughout. The tungsten electrode was ground to a 30 deg tip angle. Arcs were initiated by touch starting with an electrode from the same batch.

Argon and helium were used as shielding gases at flow rates of 30 cfh. Also, a gas mixture of 99 pct Ar-1 pct O_2 was used to investigate the effect of a small amount of oxygen on vapor concentrations.

In order to determine the composition of any vapors emitted by the tungsten electrodes, low current arcs were struck between two electrodes of the same batch.

The effects of polarity on vapor concentrations were also investigated. Spectra were recorded from arcs in straight and reverse polarity welds, as well as alternating current welds.

IV. RESULTS AND DISCUSSION

A. *Spectroscopy*

1. *Republic steels*

Spectra recorded from arcs on the three Republic 304 stainless steels are shown in Figures 1, 2, and 3. The intensities of spectral lines are measured in arbitrary units, but relative line intensities in the different spectra in this paper are all presented with the same scale. Note that the spectrum from W155 (Figure 1) exhibits calcium and aluminum lines, although this steel contains very small amounts of these elements: 4 ppm and 70 ppm, respectively. Manganese, chromium, iron, and argon lines are also visible.

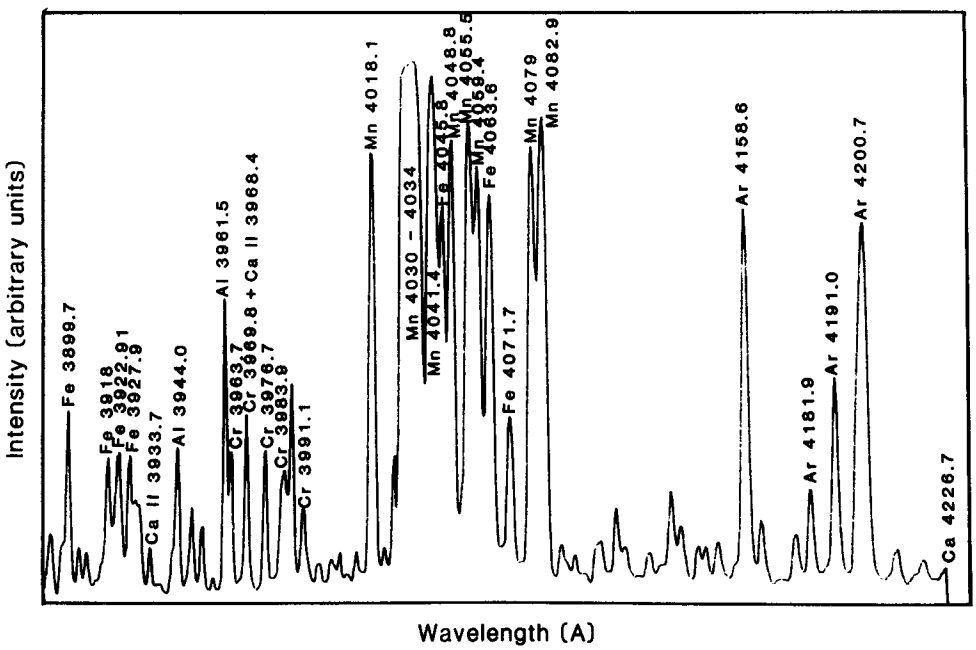

Fig. 2—Spectrum recorded from a 125 A arc on the high sulfur 304 steel (W156).

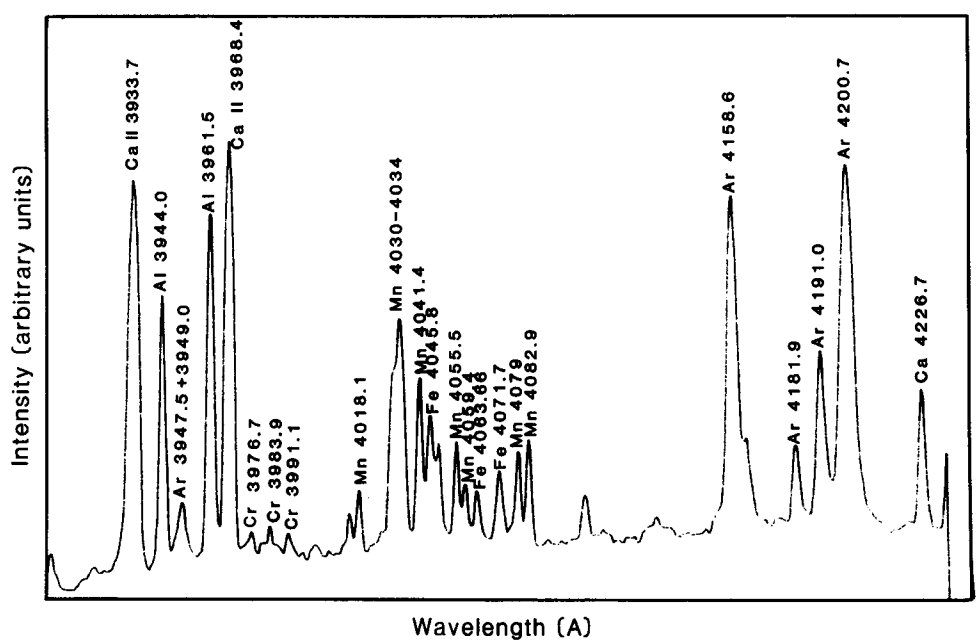

Fig. 3—Spectrum recorded from a 125 A arc on the high calcium 304 steel (W167A).

The W156 spectrum (Figure 2) contains lines from the same elements, but there are dramatic increases in the strengths of iron, manganese, and chromium lines. As the only significant compositional difference between these steels is the high sulfur content of W156, it would seem that the emission of Mn, Fe, and Cr vapors into the plasma is somehow promoted by the presence of sulfur. This conclusion was also reached by Savitski and Leskov,[6] who attributed an increase of iron and manganese vapors in the plasma to the formation of sulfides with low thermal reaction and sublimation effects. Another possible explanation for the case of manganese is that this element forms sulfide compounds which are highly surface active, thereby increasing the concentration of manganese on the weld pool surface. This would lead to increased vaporization of manganese into the welding arc.

It is interesting to note that these results conflict with those of Mills,[22] who found that enhanced Mn vaporization corresponded to steels which exhibited decreased weld penetration. W156 was found to exhibit increased weld penetration. This indicates that the presence of metal vapor in the arc is of secondary importance, and that surface tension related effects such as those described by Heiple and Roper[24-27] are dominant in controlling weld behavior.

The W167A spectrum (Figure 3) contains greatly increased calcium and aluminum lines. This is to be expected for calcium, because this steel contains twenty times more calcium than W155, but the aluminum content of W167A (90 ppm) is only slightly higher than that of W155 (70 ppm). This indicates that the emission of aluminum vapor into the plasma is somehow linked to that of calcium. This is further substantiated by in-progress observations of the weld spectrum on the X-Y oscillographic monitor: the calcium and aluminum lines are subject to severe intensity fluctuations at a frequency between 0.1 and 10 Hz while the weld is in progress, and the lines for both elements were observed to fluctuate always in unison; *i.e.*, an increase in the amount of Ca vapor in the arc was always accompanied by an increase in Al vapor. It is possible that calcium and aluminum form a surface active compound, and therefore the two elements will segregate to the surface of the weld pool and evaporate simultaneously. Another possible explanation is that calcium and aluminum are present in the metal in the form of an intermetallic compound: as the precipitate is drawn to the surface of the molten weld pool, simultaneous increases in the concentrations of calcium and aluminum vapors in the plasma will be observed. However, as discussed in the next section, simultaneous emission of Ca and Al from tungsten electrodes were also observed. Neither of the above hypotheses can explain the presence of Ca and Al vapors emanating from the electrode.

2. *Vapors emitted by the tungsten electrode*

Inconsistencies in the levels of calcium and aluminum lines in spectra of arcs on the same base plate suggested that these elements could be entering the plasma from another source. Electrode manufacturers' specifications indicated calcium and aluminum contents of less than 2 ppm. However, when spectra were recorded from arcs between two electrodes, calcium and aluminum lines were evident. Figure 4 is a spectrum recorded from a 20 A arc between two tungsten electrodes. Due to the low current, and hence lower arc temperature, the sensitive calcium ion lines at 3933 and 3968 Å are lesser in magnitude than those in the weld spectra, but the calcium neutral atom line at 4227 Å is not as greatly reduced. Spectra were also recorded from arcs on a water-cooled copper anode with the same results. It is evident from these results that a significant portion, but not all, of the calcium and aluminum vapors observed in the welding arc may originate from the tungsten electrode.

SEM/EDAX analysis of the electrode was performed to investigate the possibility of ceramic inclusions or other contamination introduced during the grinding process. None was found. Also, a metallic gas cup was used in place of the ceramic cup to determine whether some Ca or Al contamination could originate from that source. No change in weld spectra was observed.

3. *Effect of shielding gas composition*

An addition of 1 pct oxygen to the shielding gas was observed to widen the arc appreciably, and to cause the weld

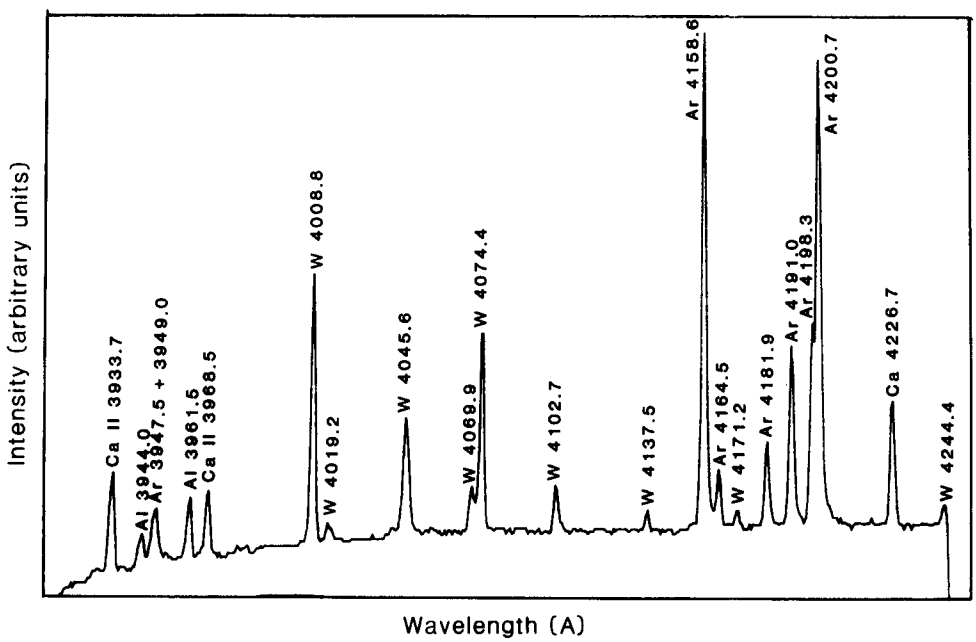

Fig. 4—Spectrum recorded from a 20 A arc between two tungsten electrodes.

pool to oscillate rapidly, indicating an unstable arc. Analysis of spectra recorded from an arc before and after this oxygen addition reveals that the addition of oxygen results in a diminishing of calcium, manganese, and aluminum lines, and a dramatic intensification of tungsten lines. This was confirmed by spectra taken from an arc between tungsten electrodes, in which the addition of oxygen rendered even the weakest lines in the tungsten spectrum detectable. This phenomenon is no doubt due to the formation of the volatile tungsten oxide, WO_3. Manganese, aluminum, and calcium, on the other hand, form more stable oxides, and therefore the amount of vapors of these elements in the arc can be expected to decrease with the addition of oxygen to the shielding gas.

4. *Effects of reverse polarity and alternating current*

Rapid fluctuations in line intensities were observed during reverse polarity and alternating current welding. This rapid fluctuation of plasma composition may explain the poor arc stability of reverse polarity gas tungsten arcs: a build-up of positively ionized metal vapors at the cathode spot will be dispersed by plasma jets, the cathode spot will immediately move to a new area of ion concentration, and so on. This movement of the cathode spot will result in arc instability.

Figure 5 shows a spectrum recorded at the moment of a sudden increase in the concentration of thorium vapor in the plasma. Virtually the entire thorium spectrum is distinguishable. Because thorium lines are not very strong, this

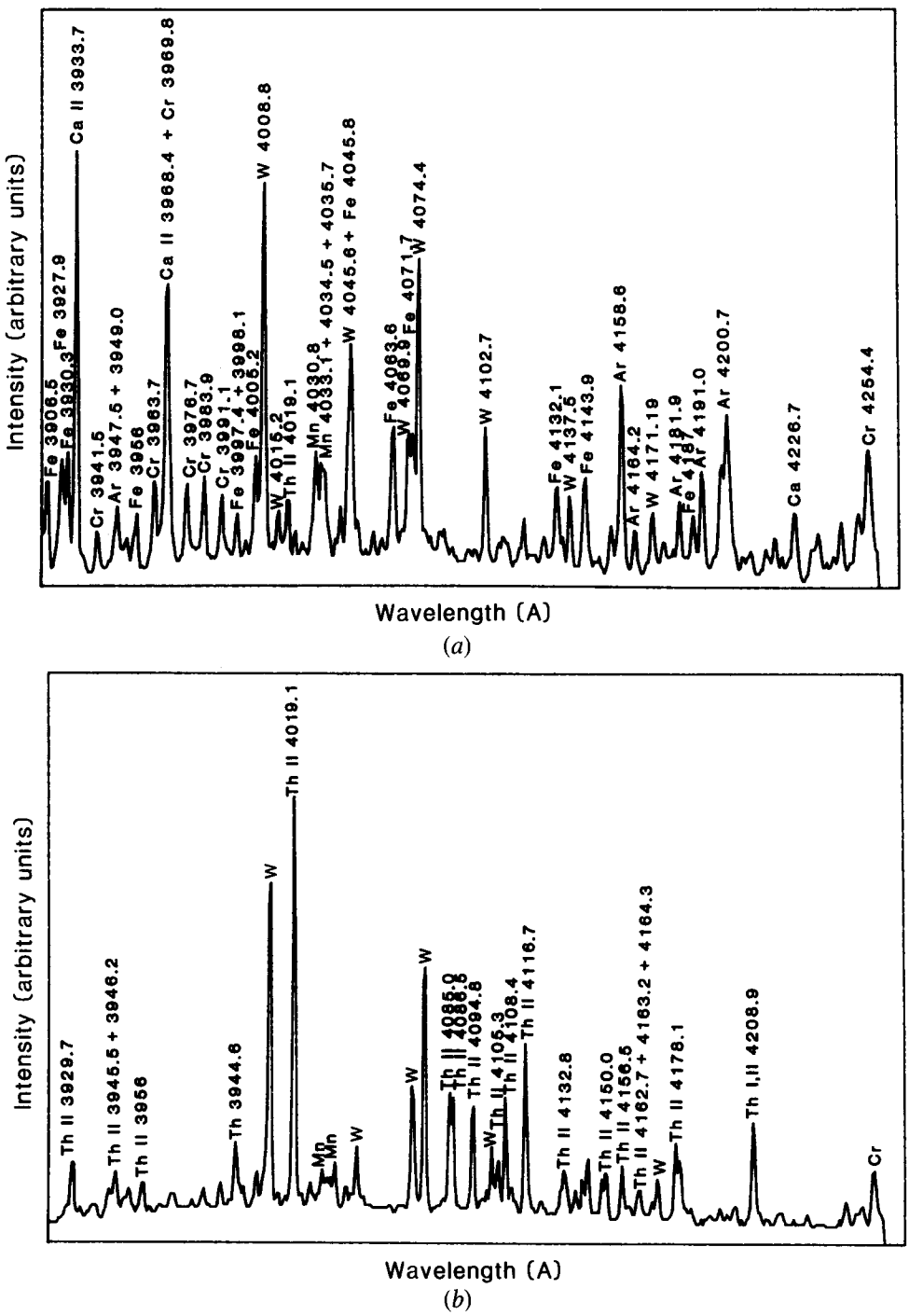

Fig. 5—Two spectra recorded from a reverse polarity 20 A arc (electrode region masked) on the high sulfur 304 steel (W156). The thorium lines fluctuated from low intensity (*a*) to high intensity (*b*).

indicates a very high concentration of thorium vapors in the electrode region.

B. *Monochromatic Photography*

A monochromatic photograph taken at 4200 Å, a characteristic wavelength of neutral argon, is shown in Figure 6(a). As can be expected, argon is distributed throughout the plasma, and accounts for a major portion of the radiation emitted by the welding arc. Figure 6(b) shows that the bright spot at the cathode normally observed in arcs is due to argon ion lines. This bright spot, also visible in monochromatic photographs by Shaw,[19] is discussed by Tsai.[33] Electrons accelerated across the cathode fall region collide with ions and are thermalized. This heat is distributed in a very small region of the arc which Tsai considers as an external heat source. The high temperature of this region will result in increased ionization, as shown in these photographs.

This phenomenon was further investigated in arcs between two tungsten electrodes and in reverse polarity arcs on a water-cooled copper plate. In the latter case, the bright spot at the tungsten electrode disappeared, and a more diffuse bright spot was evident at the copper plate. In the former case, a single bright spot appeared at the cathode only. These results confirm that this is a cathode-related rather than electrode-related phenomenon.

Photographs of arcs in mixtures of argon and helium are shown in Figures 7 through 9. Figures 7 and 8 show that, as can be expected, the intensities of argon atom and ion lines diminish with decreasing argon content. Figure 9 shows a bright spot due to helium atom emission which increases in size with increasing helium content. Due to its high ionization potential, helium will not be as highly ionized in this region, and the arc current in helium-argon mixtures will be produced primarily by argon ions and electrons. Thus, radiation from argon ions and excited helium atoms is observed in this region, while radiation from argon atoms and helium ions is not. The large size of this bright spot in helium can be attributed to helium's high thermal conductivity.

Note that light was still detected at the helium wavelength even when no helium was present in the shielding gas. This light is due to characteristic argon lines, which are very numerous. For this reason it was difficult to examine light from metallic vapors in the plasma, as interference from the complex argon spectrum is usually unavoidable due to the 14 Å minimum halfbandwidth of the monochromator. This is illustrated in Figure 10, which shows an arc on Republic W156 at 4030 Å, a characteristic Mn wavelength. It can be seen that manganese provides additional light across the surface of the weldpool, but argon light (Ar I 4032.97, 8053.31, 8066.60; Ar II 4033.82, 4035.46) is also detected. This accounts for the light in the upper part of the arc. Manganese is the most easily detected of the metals, as its four most intense lines (4030, 4033, 4034, and 4035) all lie within the 14 Å halfbandwidth of the instrument. The combined radiation at these wavelengths produces a good image. Other elements were not usually detectable over the argon "background". This problem was eliminated by switching to helium shielding gas. Helium has a far less complex spectrum than argon.

Figure 11 shows photographs of an arc on W156 at iron, chromium, calcium, calcium ion, aluminum, and aluminum ion characteristic wavelengths. The aluminum ion line at 6201 Å is closer to the infra-red end of the spectrum than the other lines studied, and therefore a greater amount of incandescence from the tungsten electrode is recorded.

It is evident from these photographs that all metal vapors in the arc are concentrated just above the weld pool surface.

Metal vapors in 25 A arcs exhibit different behavior, as shown in Figure 12. It can be seen that the vapors are present not only at the weld pool surface, but also in the upper regions of the arc. The observed distribution of metal vapors is probably due to plasma jets, as illustrated in Figure 13. At low currents, these jets will cause the metal vapors to flow to the weld pool perimeter, where they will rise due to electrostatic attraction and subsequently con-

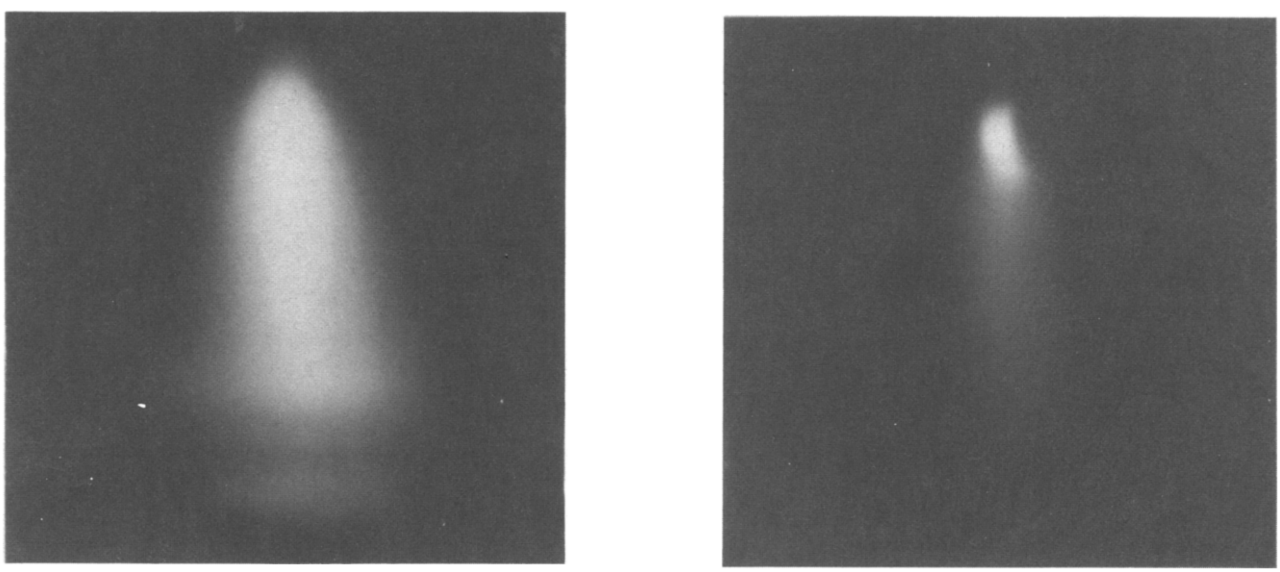

(*a*) (*b*)

Fig. 6—Monochromatic photographs of a 125 A arc on stainless steel at characteristic wavelengths of the (*a*) argon atom and (*b*) argon ion (Ar II).

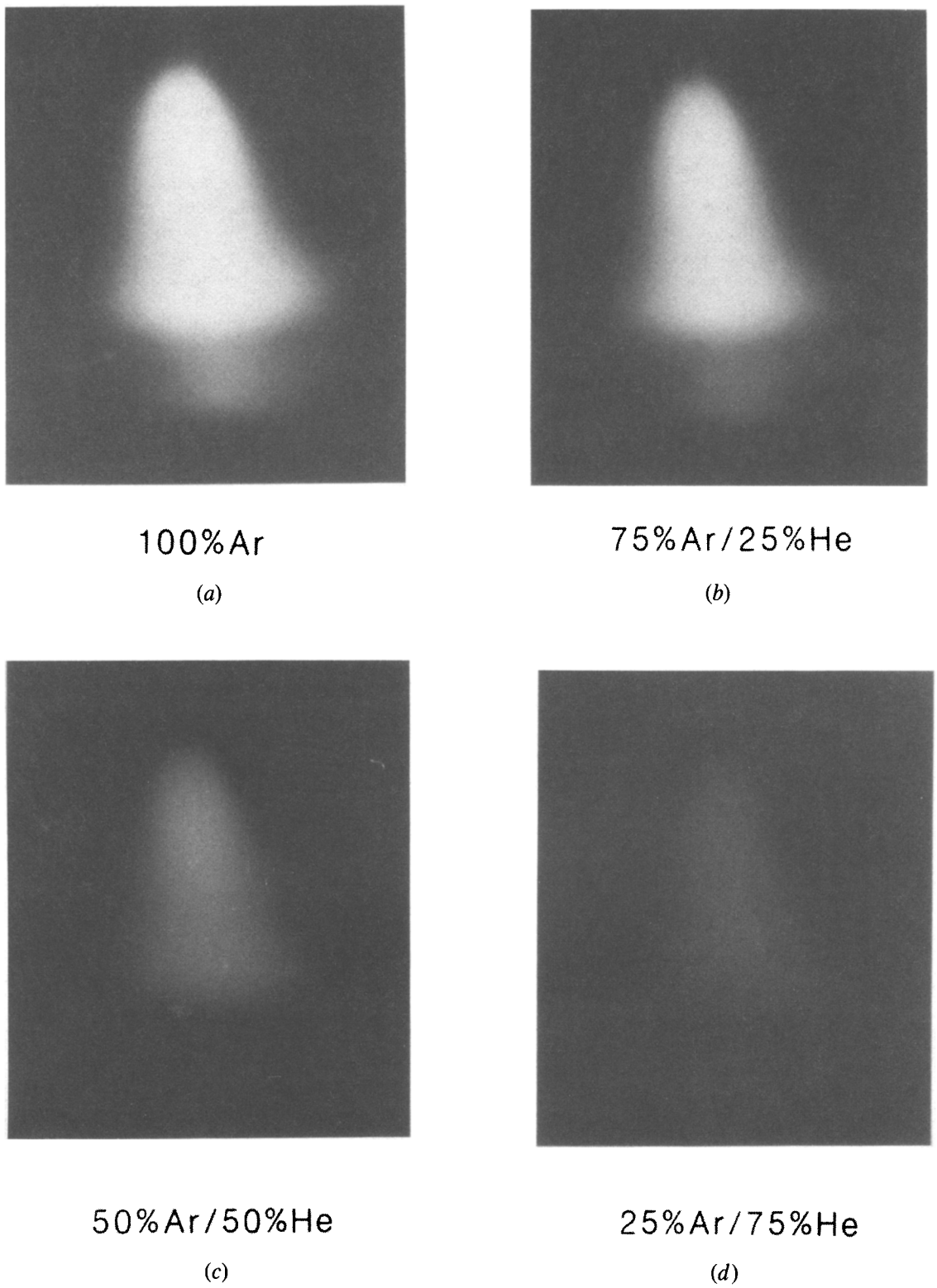

Fig. 7 — Monochromatic photographs at argon atom characteristic wavelengths of 125 A arcs on stainless steel with various Ar/He shielding gas compositions.

dense on the electrode surface. They may vaporize again from the electrode, resulting in a concentration of metal vapors in the upper region of the arc, as observed in the photographs. At higher currents, stronger jets and a larger weld pool will result in a wider dispersion of the vapors, and condensation on the electrode tip is less likely to occur. Thus, the presence of metal vapors in the upper region of high current arcs is not observed. The concentration of manganese vapor at the tungsten electrode is particularly high, and can be correlated with the manganese-rich "halo" formations observed to form on the tungsten electrode.[33]

V. CONCLUSIONS

Argon, iron, chromium, manganese, calcium, aluminum, tungsten, and thorium lines have been identified in spectra

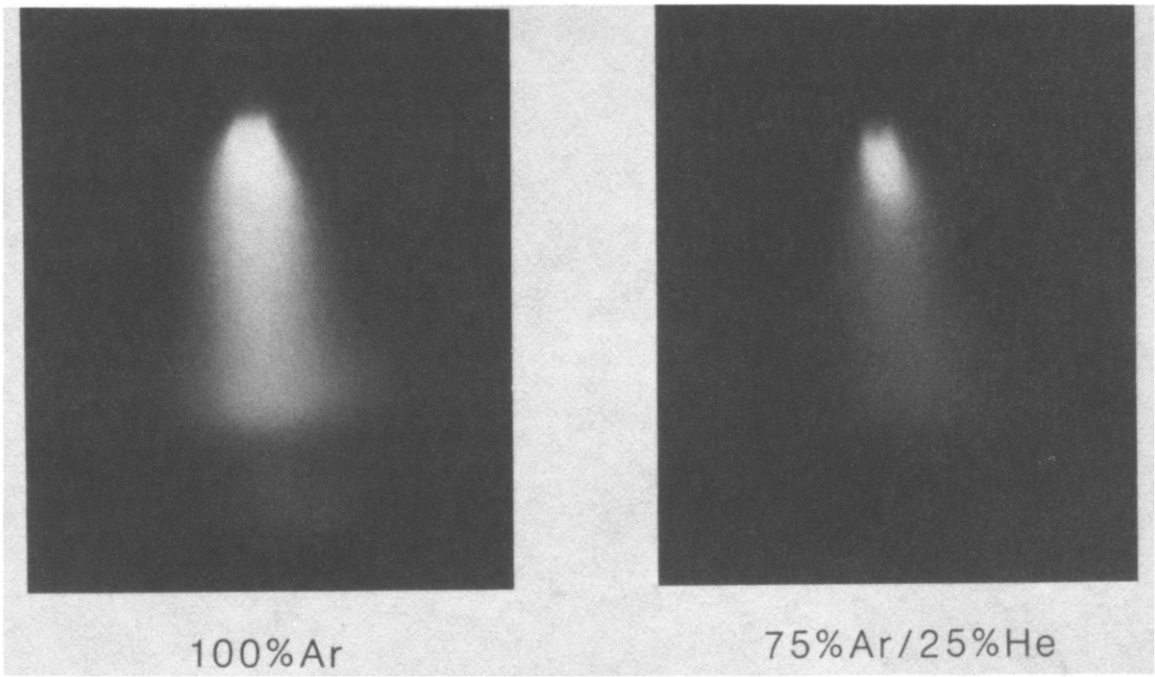

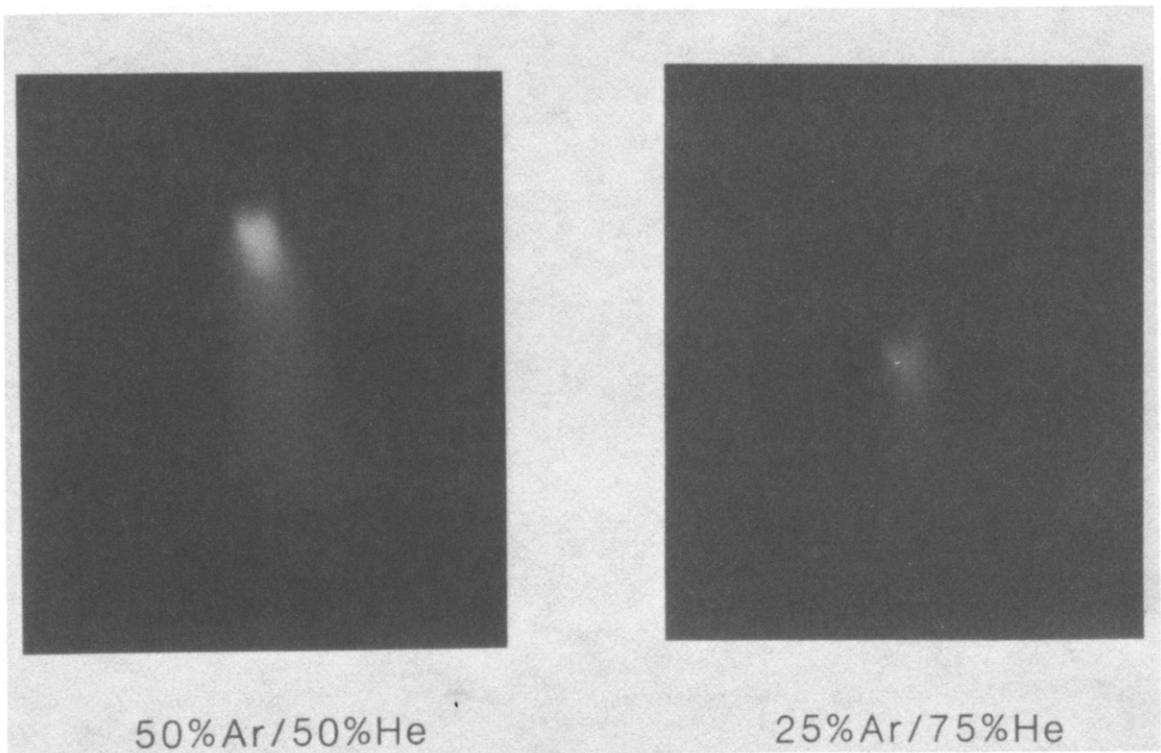

(*c*) (*d*)

Fig. 8—Monochromatic photographs at argon ion characteristic wavelengths of 125 A arcs on stainless steel with various Ar/He shielding gas compositions.

recorded from GTA welds on stainless steel. The following observations have been made:

1. The presence of sulfur in the base plate appears to promote evaporation of manganese and iron, as previously reported by Savitskii and Leskov,[6] and chromium. It is believed that this is due to the formation of sulfides which have low thermal reaction and sublimation heat effects or which are highly surface active.
2. This study found enhanced Mn evaporation in arcs on steels which exhibit increased penetration. This is in con-

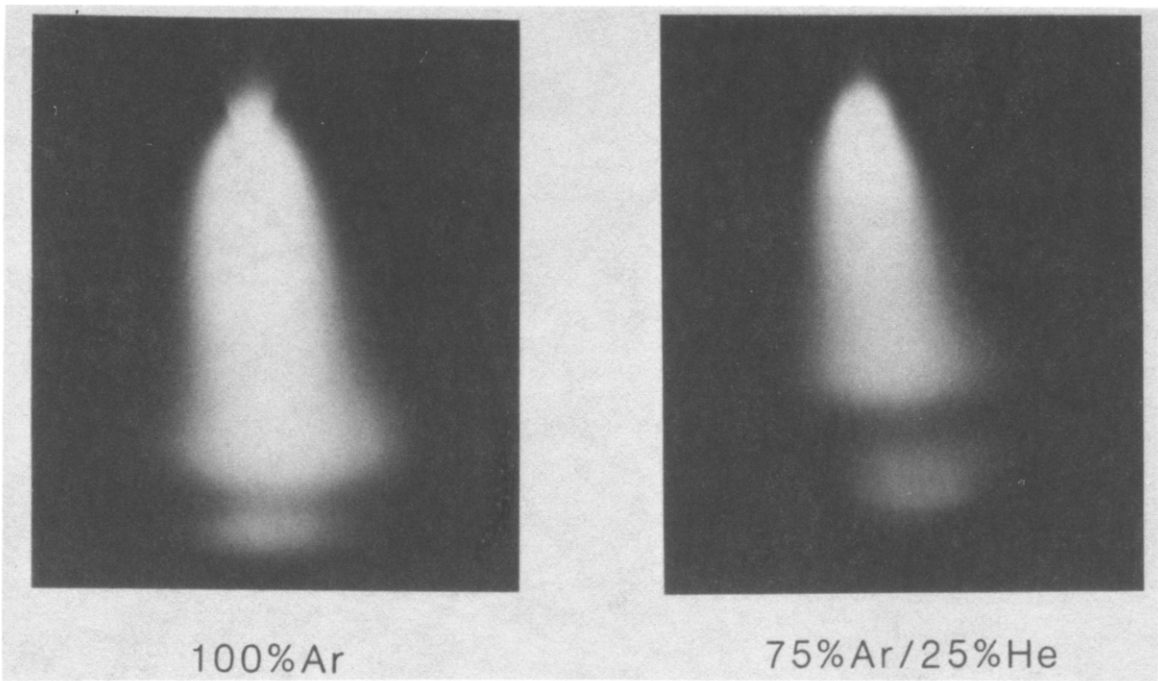

(*a*) (*b*)

(*c*) (*d*)

Fig. 9—Monochromatic photographs at helium atom characteristic wavelengths of 125 A arcs on stainless steel with various Ar/He shielding gas compositions.

flict with the results of Mills,[22] which suggests that the presence of metal vapor in the arc is of secondary importance in determining weld penetration, and that surface tension effects as described by Heiple and Roper[24–27] are more important.

3. The presence of calcium in the base plate appears to promote evaporation of aluminum. The reason for this is unclear.
4. Calcium and aluminum are detectable in the arc even when they are present only in minute amounts in the base plate. These elements were also detected in arcs between tungsten electrodes in which they are present at only a

Fig. 10—Monochromatic photograph of a 125 A arc on the high sulfur 304 steel (W156) at a manganese characteristic wavelength (argon shielding gas).

few parts per million concentration. The significance of this finding is discussed in Part II of this paper.

5. The addition of oxygen to the shielding gas results in a decrease in the concentration of calcium, manganese, and aluminum vapor in the arc, and a dramatic increase in the concentration of tungsten vapor. This is due to differences between vapor pressures of metals and their oxides.
6. Reverse polarity and alternating current arcs were observed to contain rapidly fluctuating amounts of metal vapors. This may account for the poor stability sometimes encountered in these arcs.

A method of monochromatic photography has been developed which provides an extremely high filter rejection ratio and thus allows filming of the location of metal vapors in gas tungsten arcs. It has been found that, in order to eliminate the interference of the complex argon spectrum, helium shielding gas must be used. It has been shown that the metal vapors are concentrated in a region of the arc just above the weld pool. It appears that plasma jets cause these vapors to rise along the arc periphery to the upper regions of the arc, where they may condense in "halo" formation on the electrode tip.

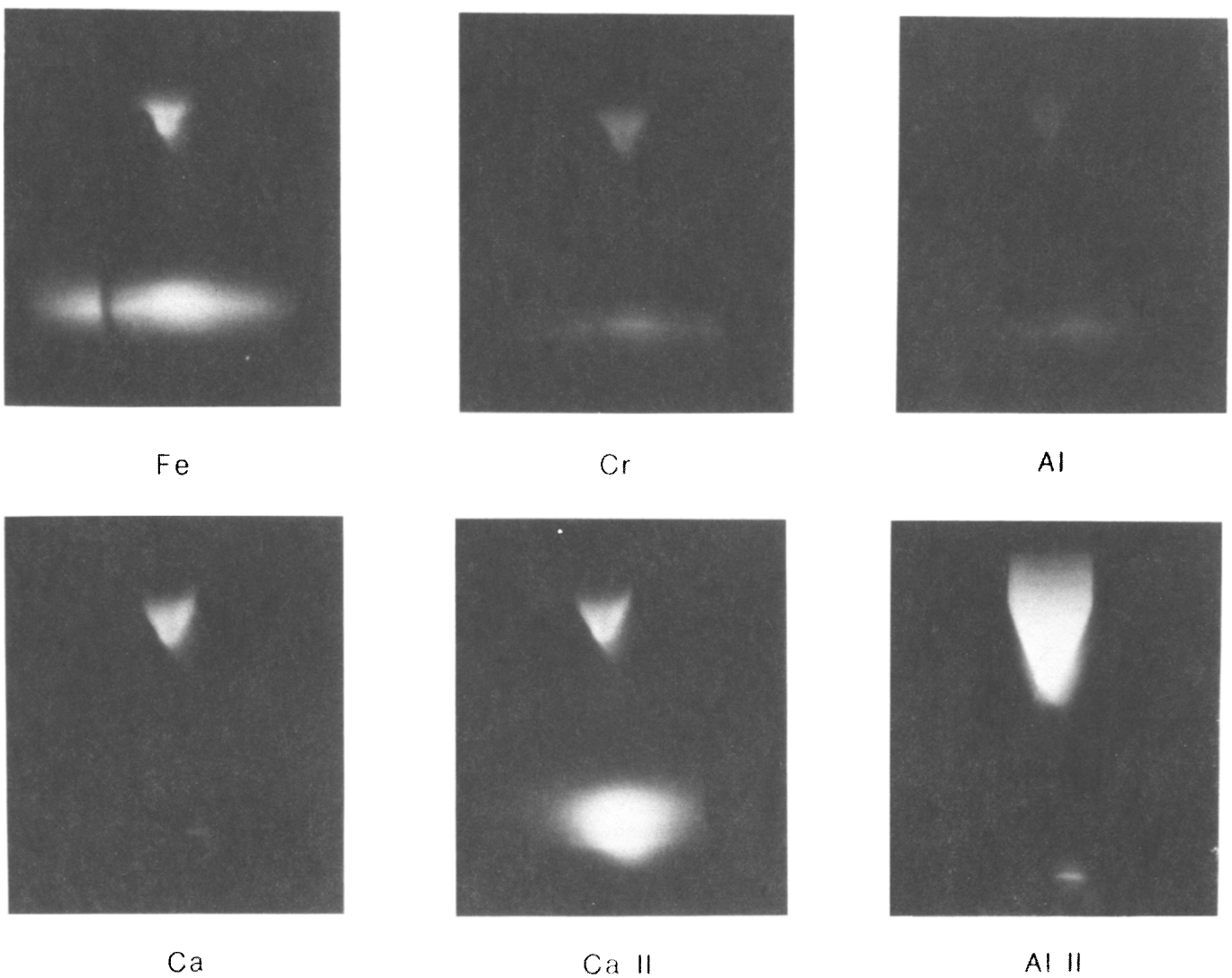

Fig. 11—Monochromatic photographs of a 125 A arc on the high sulfur 304 steel (W156) at characteristic wavelengths of the indicated species (helium shielding gas).

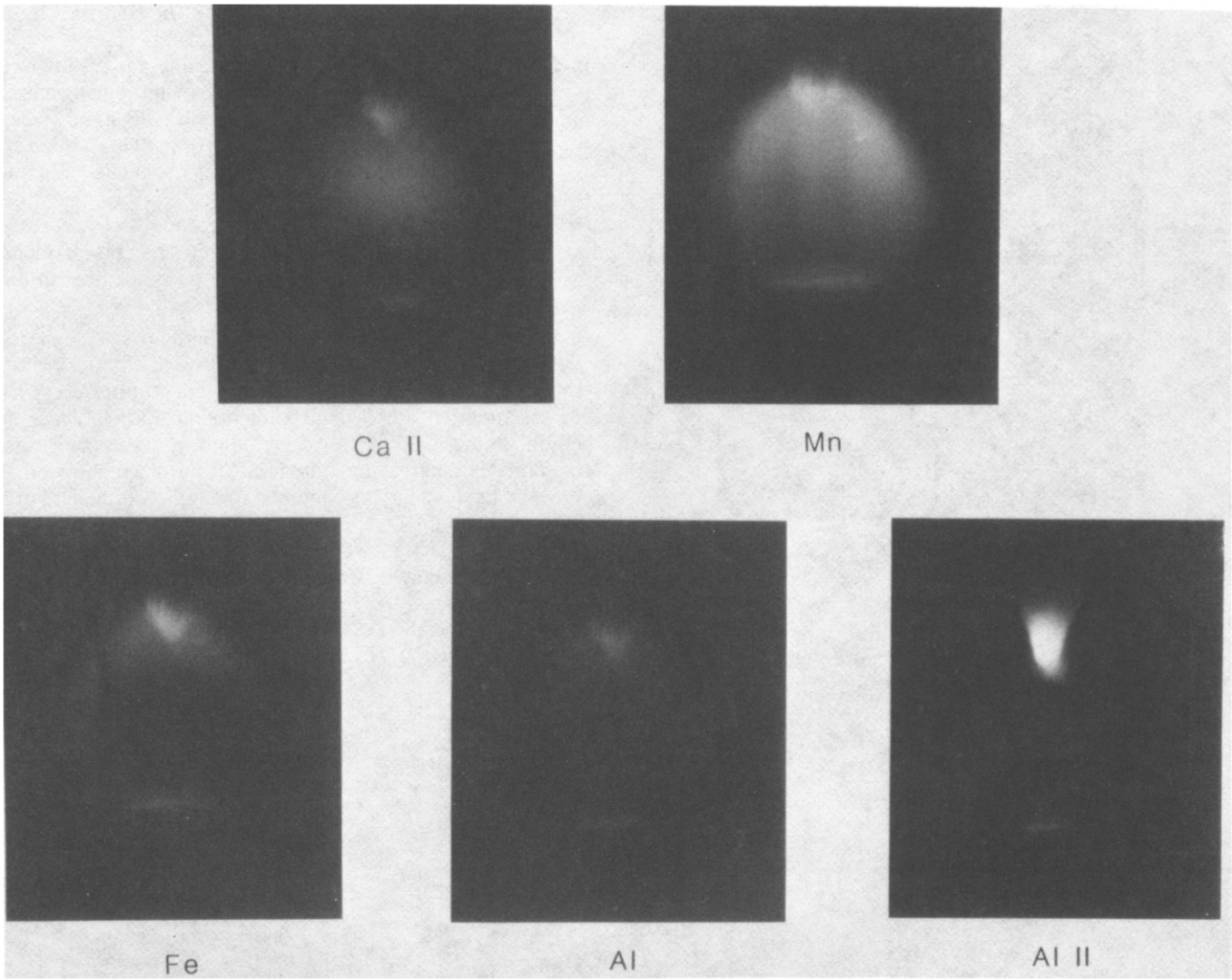

Fig. 12—Monochromatic photographs of a 25 A arc on the high sulfur 304 steel (W156) at characteristic wavelengths of the indicated species (helium shielding gas).

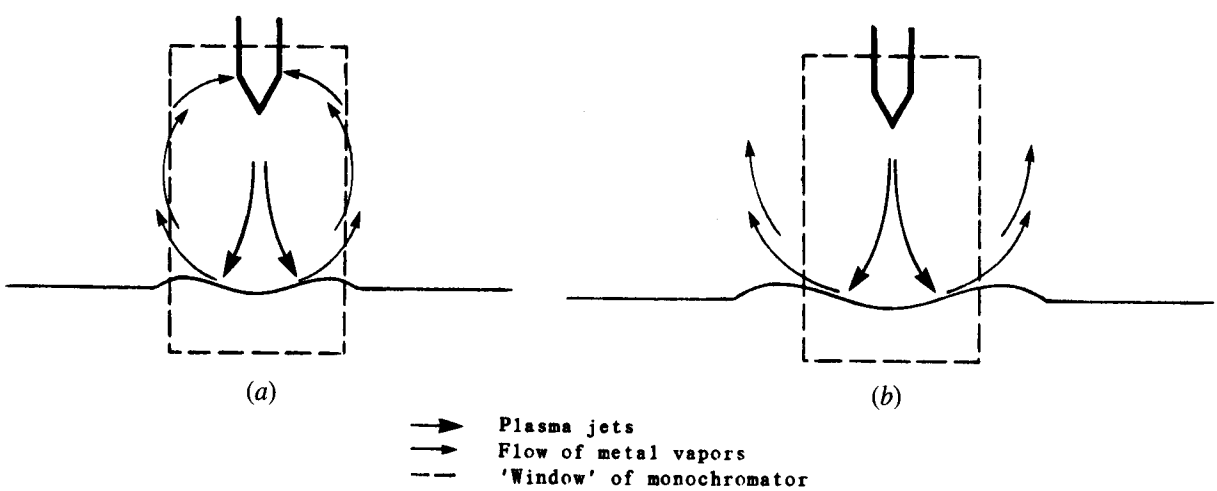

Fig. 13—Diagram of the effects of plasma jets on metal vapor flow for (*a*) low currents and (*b*) high currents.

The effects of these vapors on arc properties remain to be shown. This will be discussed in Part II of this work.

ACKNOWLEDGMENTS

The authors gratefully acknowledge the support of the Office of Naval Research under Contract No. N00014-80-C-0384. They are also indebted to Dr. D. W. Dickenson, formerly of Republic Steel Corporation, for providing the three experimental stainless steels, and Dr. Gordon Hunter for help in preparing this paper.

REFERENCES

1. S. S. Glickstein and W. Yeniscavich: *Welding J.*, 1977, vol. 56, pp. 1-18.
2. H. C. Ludwig: *Welding J.*, 1968, vol. 47, pp. 234s-40s.
3. T. Moisio and J. Leinonen: in *Arc Physics and Weld Pool Behavior*, Welding Institute, Cambridge, England, 1980, pp. 285-87.
4. J. C. Metcalfe and M. B. C. Quigley: *Welding J.*, 1977, vol. 56, pp. 133s-39s.
5. G. W. Oyler, R. A. Matuszesk, and C. R. Garr: *Welding J.*, 1967, vol. 46, pp. 1006-11.
6. M. M. Savitskii and G. I. Leskov: *Autom. Weld.*, 1980, vol. 33, no. 9, pp. 11-16.
7. W. S. Bennett and G. S. Mills: *Welding J.*, 1974, vol. 53, pp. 548s-53s.
8. R. A. Patterson: *Welding J.*, 1978, vol. 57, pp. 383s-86s.
9. D. W. Dickinson: Republic Steel Corp., Independence, OH, unpublished research, 1981-83.
10. T. F. Chase, Jr. and W. F. Savage: *Welding J.*, 1971, vol. 50, pp. 467s-73s.
11. W. F. Savage, E. F. Nippes, and G. M. Goodwin: *Welding J.*, 1977, vol. 56, pp. 126s-32s.
12. W. F. Savage, C. D. Lundin, and G. Goodwin: *Welding J.*, 1968, vol. 47, pp. 313s, 322s, 336s.
13. S. S. Glickstein: in *Arc Physics and Weld Pool Behavior*, Welding Institute, Cambridge, England, 1980, pp. 1-16.
14. E. Pfender: *WRC Progress Reports*, 1982, vol. 37, no. 2, pp. 18-32.
15. A. N. Zaidel', V. K. Prokof'ev, S. M. Raiskii, V. A. Slavnyi, and E. Ya. Shreider: *Tables of Spectral Lines*, 3rd ed., IFI/Plenum, New York, NY, 1970.
16. E. Friedman and S. S. Glickstein: *Welding J.*, 1976, vol. 55, pp. 4085-4205.
17. A. Block-Bolten and T. W. Eagar: in *Trends in Welding Research*, S. A. David, ed., ASM, Metals Park, OH, 1982, pp. 53-73.
18. S. S. Glickstein: *Welding J.*, 1976, vol. 55, pp. 222s-29s.
19. C. B. Shaw, Jr.: *Welding J.*, 1975, vol. 54, pp. 33s-44s.
20. J. F. Key, M. E. McIlwain, and L. Isaacson: in *Sixth International Conference on Gas Discharges and Their Applications*, Conf. Publ. No. 189, part 2, Institution of Electrical Engineers, New York, NY, 1980, pp. 235-38.
21. M. B. C. Quigley, P. H. Richards, D. T. Swift-Hook, and A. E. F. Glick: *J. Phys. D.*, 1973, vol. 6, pp. 2250-58.
22. G. S. Mills: *Welding J.*, 1979, vol. 58, pp. 21s-24s
23. O. N. Ivanova: *Autom. Weld.*, 1968, vol. 21, no. 2, pp. 12-15.
24. C. R. Heiple and J. R. Roper: *Welding J.*, 1981, vol. 60, pp. 143s-45s.
25. C. R. Heiple and J. R. Roper: *Welding J.*, 1982, vol. 61, pp. 97s-102s.
26. C. R. Heiple and J. R. Roper: in *Trends in Welding Research in the United States*, S. A. David, ed., ASM, Metals Park, OH, 1982, pp. 489-520.
27. C. R. Heiple, J. R. Roper, R. T. Stagner, and R. J. Aden: *Welding J.*, 1983, vol. 62, pp. 72s-77s.
28. A. M. Makara, M. M. Savitskii, B. N. Kushnirenko, N. I. Varenko, A. D. Mel'nik, D. N. Ganelin, and A. M. Toschev: *Autom. Weld.*, 1977, vol. 30, no. 9, pp. 1-3.
29. R. E. Sundell: General Electric Co., Schenectady, NY, unpublished research, 1983-84.
30. Y. Arata, S. Miyake, H. Matsuoka, and H. Kishimoto: *Trans. JWRI*, 1981, vol. 10, pp. 33-38. (Note: this report neglects aberrations inherent to the spectrograph, and therefore attributes all aberrations to the SIT detector.)
31. C. Allemand: *Appl. Optics*, 1983, vol. 22, pp. 16-17.
32. E. W. Kim and C. D. Allemand: MIT, Cambridge, MA, unpublished research, 1985.
33. N. S. Tsai: Doctoral Thesis, MIT, Cambridge, MA, June 1983.
34. S. S. Glickstein, E. Friedman, and W. Yeniscavich: *Welding J.*, 1975, vol. 54, pp. 113s-22s.